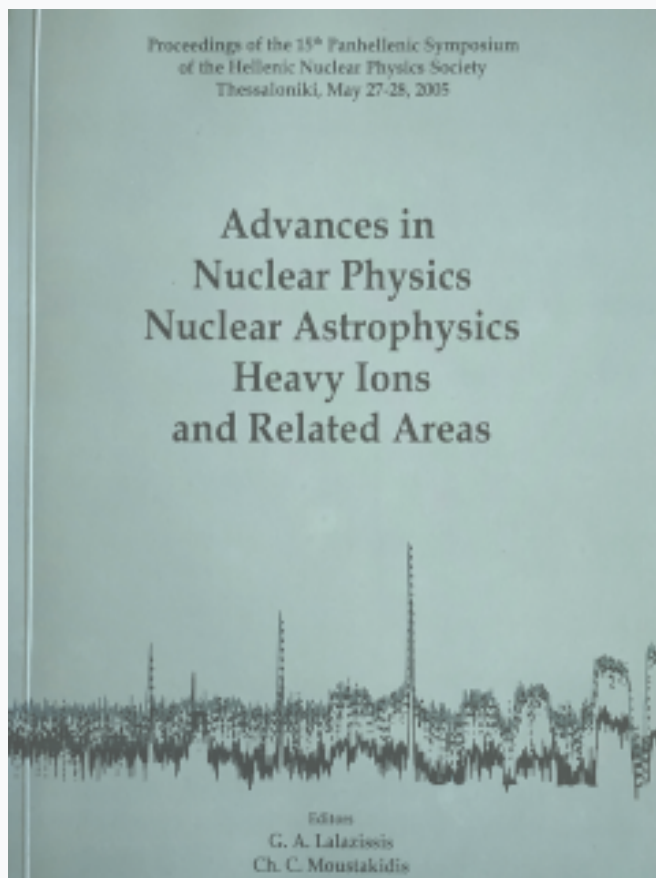


## HNPS Advances in Nuclear Physics

Vol 14 (2005)

HNPS2005



### Phase Space Analysis of Relaxation Dynamics of Isoscalar Giant Monopole Resonances

*P. K. Papachristou, E. Mavrommatis, V. Constantoudis, F. K. Diakonou, J. Wambach*

doi: [10.12681/hnps.2261](https://doi.org/10.12681/hnps.2261)

#### To cite this article:

Papachristou, P. K., Mavrommatis, E., Constantoudis, V., Diakonou F. K., & Wambach, J. (2019). Phase Space Analysis of Relaxation Dynamics of Isoscalar Giant Monopole Resonances. *HNPS Advances in Nuclear Physics*, 14, 131–136. <https://doi.org/10.12681/hnps.2261>

# Phase Space Analysis of Relaxation Dynamics of Isoscalar Giant Monopole Resonances

P.K. Papachristou<sup>a</sup> E. Mavrommatis<sup>a</sup> V. Constantoudis<sup>b</sup>  
F.K. Diakonos<sup>a</sup> J. Wambach<sup>c</sup>

<sup>a</sup>*Department of Physics, University of Athens*

<sup>b</sup>*Institute of Microelectronics (IMEL), NCSR "Demokritos"*

<sup>c</sup>*Institut für Kernphysik, Technische Universität Darmstadt*

---

## Abstract

A classical model based on the independent particle approach to the nuclear dynamics is used to study the influence of the phase space structures on the one-body dissipation of isoscalar Giant Monopole Resonances. The model consists of a harmonic oscillator describing the collective excitation coupled with a nonlinear (Woods-Saxon) oscillator representing the motion of each nucleon. We are particularly interested in the dependence of relaxation on the energy of the system. We have found that in a rather broad region of parameter space, contrary to the common expectation, both Lyapunov exponent and relaxation time increase as a function of the total energy. We examine the conditions required for this effect to occur and demonstrate the key role of the dispersion relation of the nonlinear oscillator.

---

## 1 Introduction

There is continuous interest, both theoretical and experimental, in the study of the relaxation of nuclear giant resonances (1; 2; 3; 4; 5; 6; 7). There are many relaxation mechanisms, such as one and two body dissipation, collisional damping etc. Dynamics in nuclear systems, including giant resonances, is usually mixed, i.e. regular and chaotic regions coexist in phase space (3; 4; 5; 6; 7). The effect of chaotic dynamics on their damping is still not completely understood. In general, the largest Lyapunov exponent ( $\lambda_1$ ) is the most common measure of the chaoticity of the system. It appears that, at least in completely chaotic systems, increasing  $\lambda_1$ , the relaxation time, defined as the time required for an observable to reach its equilibrium value, decreases (8). However, in mixed systems the relationship between  $\lambda_1$  and relaxation time is not well established yet.

We have employed a simple classical model based on the independent particle approach for the dynamics of the nucleons (9). This model can be used for the determination of the decay mechanisms of the isoscalar monopole resonance (the breathing mode) (2; 3; 4; 6; 7). It consists of a harmonic oscillator describing the collective excitation (to a first approximation) coupled with a nonlinear (Woods-Saxon) oscillator. The model corresponds to a time-independent Hamiltonian system with 2 degrees of freedom exhibiting mixed dynamics. Our aim is to explore the interrelation between the relaxation time of the harmonic oscillator and  $\lambda_1$  and how this is affected by changes in the chaotic fraction of phase space. In Sec. 2 we describe our model. In Sec. 3 we present our main findings. In Sec. 4 we discuss the dependence of our findings on some of the parameters. In Sec. 5 we summarize our main results and give future prospects.

## 2 Description of the model system

Our model system consists of a particle of mass  $m$  moving in a Woods-Saxon well of finite depth  $V_o$  coupled with a harmonic oscillator of mass  $M$  moving with frequency  $\omega_{HO}$ . The Hamiltonian of the system is

$$H = \frac{p_r^2}{2m} - \frac{V_o}{1 + \exp\left(\frac{r-R_o+b(R_o-R)}{a}\right)} + \frac{p_R^2}{2M} + \frac{1}{2}M\omega_{HO}^2(R - R_o)^2. \quad (1)$$

The choice of this Hamiltonian is motivated by the study of the damping of Isoscalar Giant Monopole Resonances (IGMR) in nuclei. Specifically, this mode is represented by a harmonic oscillator which interacts with the nucleons, represented as independent particles moving in an average potential which has the form of a Woods-Saxon well. The strength of the coupling between the particle and the harmonic oscillator is controlled by the parameter  $b$ . In the limit  $b \rightarrow 0$  the oscillators become uncoupled and thus the system becomes integrable. As  $b$  increases the system becomes increasingly chaotic. In nuclear systems  $b$  equals to 1 and the coupling is adjusted by the ratio  $M/m$ .

## 3 Relaxation time, Lyapunov exponent and chaotic fraction of phase space

For the analysis of the system dynamics, we start with a microcanonical ensemble of initial conditions in a rectangular region of  $(r, E_p)$  plane, where  $E_p$  is the particle energy. For each such ensemble, the total energy  $E$  is constant. All initial conditions we use belong to the main chaotic region of phase space. We

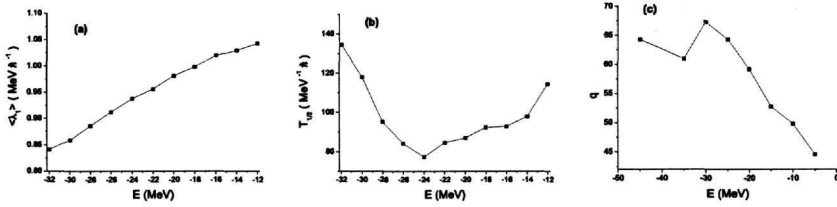


Fig. 1. (a)  $\langle \lambda_1 \rangle$ , (b)  $T_{1/2}$  and (c)  $q$  as a function of the total energy  $E$  for  $M/m = 1$ ,  $R_0 = 7.69 fm$ ,  $a = 0.05 fm$ ,  $V_0 = 48 MeV$ ,  $\omega_{HO} = 13.73 MeV/\hbar$  and  $b = 0.08$ .

evolve them forward in time and at each time instant  $t$  we calculate the mean value  $\langle R(t) \rangle$  of the coordinate  $R$  of the harmonic oscillator. It is expected that  $\langle R(t) \rangle$  will approach the equilibrium value  $R_{eq} \simeq R_0$  almost exponentially (8), since all orbits in the ensemble are chaotic. The corresponding time scale defines the relaxation time. For the values of the parameters chosen, the time dependence of  $\langle R(t) \rangle - R_{eq}$  can be fitted very well by a function of the form  $R - R_{eq} = Ae^{-\gamma t} \cos(\omega t)$ . We calculate the half-life  $T_{1/2}$  of the initial amplitude  $A$  as a function of the total energy of the system. To quantify the degree of chaoticity of these orbits, we calculate for each one the Lyapunov exponent  $\lambda_1$ . We determine the average value  $\langle \lambda_1 \rangle$  over the ensemble of initial conditions as a function of the total energy of the system. In addition to  $\lambda_1$  we calculate the percentage  $q$  of chaotic phase space in the  $(R, p_R)$  plane as a function of the total energy of the system. In the study presented in this section we choose the following values for the parameters of the system:  $R_0 = 7.69 fm$ ,  $V_0 = 48 MeV$  and  $\omega_{HO} = 13.73 MeV/\hbar$ . These parameters are relevant for the decay of the IGMR of the nucleus  $^{208}Pb$  (2; 3; 6). The strength of the coupling has been chosen equal to  $b = 0.08$ . We also choose  $M/m = 1$  and  $a = 0.05 fm$ . The results for  $\langle \lambda_1 \rangle$ ,  $T_{1/2}$ , and  $q$  as a function of the total energy of the system are shown in Fig. 1. It is clearly seen that although the value of  $\langle \lambda_1 \rangle$  is a monotonically increasing function of the total energy  $E$ , the relaxation time, above a critical value of the total energy, starts increasing contrary to the common expectation from fully chaotic systems (8). We also observe that above this critical energy, the percentage  $q$  of chaoticity in the  $(R, p_R)$  section is decreasing. Motivated by this observation we consider in more detail the Poincaré surfaces of section for different values of the total energy of the system. In Fig. 2,  $(R, p_R)$  sections (for  $r = R_0/2$  and  $p_r > 0$ ) for three values of the total energy are shown. In Fig. 3 we plot  $(r, E_p)$  sections (for  $R = R_0$ ,  $p_R > 0$ ) for the same values of the total energy.

The regular region of Fig. 2(c) contains invariant tori and corresponds to the upper invariant curves of Fig. 3(c). These curves are close to straight lines and correspond to almost constant particle energy and hence almost constant total energy. They are therefore Kolmogorov- Arnold- Moser (KAM) tori, which are remnants of the uncoupled integrable system. By inspecting these

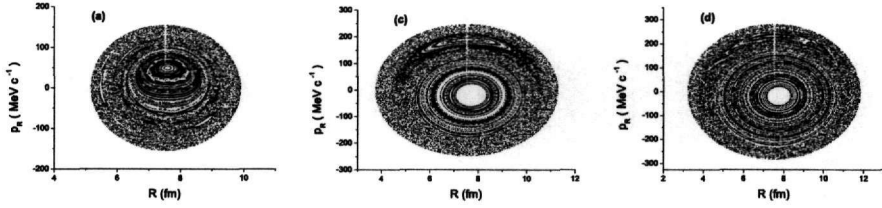


Fig. 2.  $(R, p_R)$  Poincaré sections for (a)  $E = -35\text{MeV}$ , (b)  $E = -15\text{MeV}$  and (c)  $E = -5\text{MeV}$ . For the values of the other parameters see text (Sec. 3).

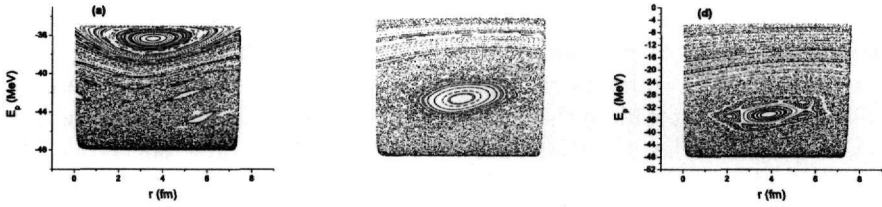


Fig. 3.  $(r, E_p)$  Poincaré sections for (a)  $E = -35\text{MeV}$ , (b)  $E = -15\text{MeV}$  and (c)  $E = -5\text{MeV}$ . For the values of the other parameters see text (Sec. 3).

Poincaré sections, we observe that the appearance of KAM tori leads to the observed relative decrease of chaos in phase space. The onset of this decrease coincides with a change in the monotonicity of  $T_{1/2}$  as a function of the energy. Once the KAM tori appear, they are not destroyed as the energy increases. We conjecture that such an appearance of KAM tori counteracts the increase of the Lyapunov exponent and leads to a change in the monotonicity of the relaxation time.

#### 4 The key role of dispersion relation and the influence of the coupling strength

The diffuseness parameter  $a$  is of crucial importance for the appearance of the effect described in the previous section. In the Woods-Saxon potential  $V_{WS}(r) = -V_0 / \left(1 + \exp\left(\frac{r-R_0}{a}\right)\right)$ , the frequency of the motion of the particle  $\omega_p$  depends on its energy  $E_p$ . The frequency of the motion of a particle in a potential  $V(r)$  is given by

$$\omega_p(E_p) = \pi \left( \int_{r_l}^{r_r} \frac{dr}{\sqrt{2(E_p - V(r))}} \right)^{-1}, \quad (2)$$

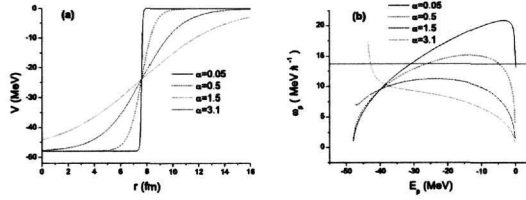


Fig. 4. (a) The Woods-Saxon potential for  $V_0 = 48 \text{ MeV}$  and four values of  $a$ , namely  $0.05 \text{ fm}$ ,  $0.5 \text{ fm}$ ,  $1.5 \text{ fm}$ , and  $3.1 \text{ fm}$ , (b) The  $\omega_p(E_p)$  curve of the Woods-Saxon potential for the same values of the  $a$ . The straight line shows the frequency of the harmonic oscillator.

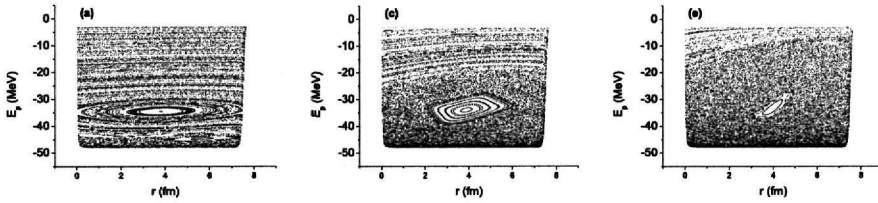


Fig. 5.  $(r, E_p)$  Poincaré sections for  $E = -5 \text{ MeV}$ ,  $a = 0.05 \text{ fm}$  and (a)  $b = 0.02$ , (b)  $b = 0.1$  and (c)  $b = 0.2$ .

where  $r_r$  and  $r_l$  are the right and left turning points at a given energy  $E_p$ . The form of the  $\omega_p(E_p)$  curve of the Woods-Saxon potential depends strongly on  $a$  as can be seen from Fig. 4, where  $V(r)$  and  $\omega_p(E_p)$  curves for four values of  $a$  are shown. At the limit  $a \rightarrow 0$  the potential tends to the square well and therefore the  $\omega_p(E_p)$  curve has the form  $\omega_p \propto \sqrt{E_p}$ . For large values of  $a$ ,  $\omega_p(E_p)$  is decreasing and for intermediate values it has a maximum.

In the following we consider a value of  $a$  (i.e.  $a = 0.05 \text{ fm}$ ) for which the above mentioned behaviour of relaxation time occurs. The  $\omega_p(E_p)$  curve has two intersection points with the corresponding curve of the harmonic oscillator. The leftmost intersection point is a  $\omega_p : \omega_{HO} = 1 : 1$  resonance which is apparent in Figs. 2 and 3. For small values of  $b$ , the phase-space is dominated by KAM tori. Resonances of small width also exist. As the coupling strength  $b$  increases, the width of these resonances also increases. They therefore overlap with higher-order resonances located close to them leading to the appearance of a chaotic region. The area of this chaotic region increases with  $b$ . Higher-order resonances ( $1 : 2$ ,  $1 : 3$ , ...) appear in the low-energy region and their density increases as the energy becomes smaller. Therefore, as  $b$  increases *chaos emerges first in the low-energy region of the  $(r, E_p)$  section*. This transition is illustrated in Fig. 5.

For fixed values of  $b$  and  $a$ , above some particle energy threshold only KAM tori exist. As the energy increases, the existing KAM tori are not destroyed

and new KAM tori are added to the phase space in the region of large particle energies. Therefore, as the energy increases, the relative area of the chaotic phase space decreases, as can be seen from Fig. 3. Increasing  $b$  makes the system more chaotic, i.e. both the Lyapunov exponent and the relative area of the chaotic phase space increase (see Fig. 5). The inverse behaviour of relaxation time and Lyapunov exponent appears as long as a sufficiently wide layer of KAM tori exists at high energies. Increasing  $b$  further, will lead to a destruction of all KAM tori and thus to the usual behaviour of the relaxation time:  $\langle \lambda_1 \rangle$  is an increasing function of the energy,  $q$  is also increasing due to the decrease of the area of the regular island around the 1 : 1 resonance and  $T_{1/2}$  is decreasing. Increasing  $a$  beyond a critical value of around 1, leads to a qualitative change in the dispersion relation. In that case chaos emerges from the region of high energies in the  $(r, E_p)$  section and the effect of the simultaneous increase of  $\langle \lambda_1 \rangle$  and relaxation time is destroyed.

## 5 Conclusions

We have studied a classical model suitable for the investigation of the decay of Isoscalar Giant Monopole Resonances (IGMRs) focusing on relaxation properties. Using phase space considerations, it has been found that, in a rather broad range of the parameters, the relaxation time can increase or remain constant although the Lyapunov exponent increases. We have attributed this behaviour to the appearance of KAM tori. For this behaviour to occur, the dispersion relation of the non-harmonic oscillator must either be strictly increasing or have a maximum. The model presented in this work is currently used for the detailed study of the decay width of IGMRs in several nuclei. The results of these studies will be presented in a forthcoming paper (10).

## References

- [1] M.N. Harakeh, Nucl. Phys. A **731** 411 (2004); A. Richter, *ibid* 59.
- [2] D. Youngblood et al., Phys. Rev. Lett. **82** 691 (1999).
- [3] G.F. Burgio et al., Phys. Rev. C **52**, 2475 (1995).
- [4] M. Baldo et al., Phys. Rev. C **58**, 2821 (1998).
- [5] S. Drozdet et al., Phys. Rev. Lett. **74** 1075 (1995).
- [6] D. Vretenar et al., Phys. Rev. E **60** 308 (1999).
- [7] G.A. Lalazissis et al., Chaos Solitons and Fractals **17** 585 (2003).
- [8] H. Kandrup and M.E. Mahon, Phys. Rev. E **49**, 3735 (1994).
- [9] P.K. Papachristou et al., submitted to Phys. Rev. E.
- [10] P.K. Papachristou et al., in preparation.